ELSEVIER

Nuclear Physics A590 (1995) 11c-28c

NUCLEAR PHYSICS A

# RHIC and QCD: an overview

T. D. Lee

Columbia University, New York, N.Y. 10027

In this talk I would like to give an overview of the central areas of quark matter physics: Relativistic Heavy Ion Collisions and Quantum Chromodynamics.

We will begin with the theme of *vacuum as a condensate* and then review RHIC physics and QCD, summarizing the present knowledge of phase transitions and QCD phase diagrams, with particular emphasis on the present theoretical limitations. Finally we will present a new theoretical approach which may remove some of these limitations. Following is an outline of the talk.

## *Two Puzzles Of Modern Physics*

Vacuum As a Condensate

## *RHIC Physics and QCD*

Phase Transitions
Present Theoretical Limitations

## *A New Theoretical Approach*

Elimination of Spurious Fermion Solutions
Noncompact Formulation of Lattice QCD

---

*This research was supported in part by the U.S. Department of Energy.


*SSDI* 0375-9474(95)00224-3

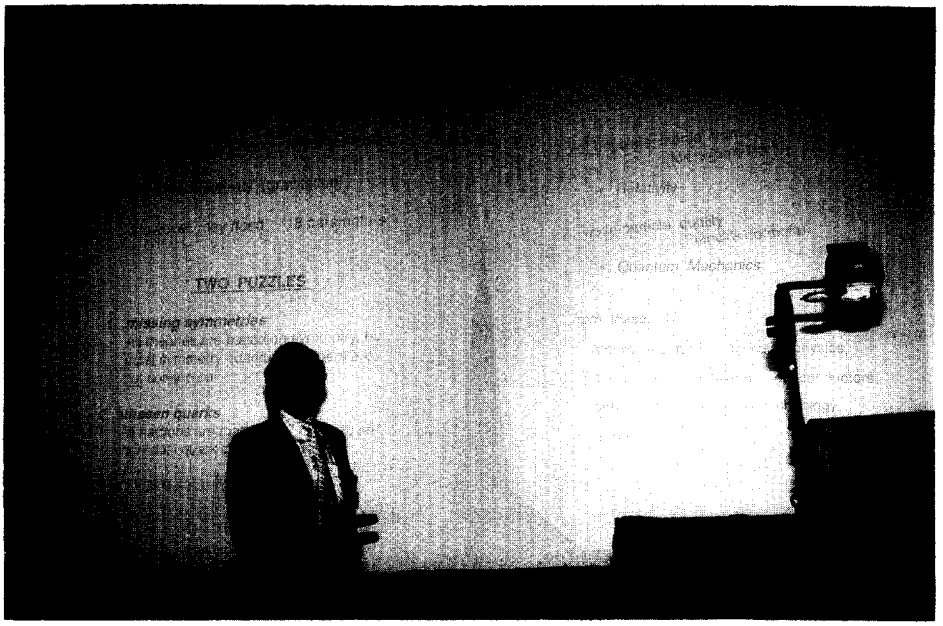


T.D. Lee

# 1. TWO PUZZLES OF MODERN PHYSICS

The status of our present theoretical structure can be summarized as follows:

**QCD** (strong interaction)
$SU(2) \times U(1)$ **Theory** (electroweak)
**General Relativity** (gravitation).

However, in order to apply these theories to the real world, we need a set of about 18 parameters, all of unknown origins. Thus, this theoretical edifice cannot be considered complete.

The two outstanding puzzles that confront us today are:

**i) Missing symmetries** - All present theories are based on symmetry, but most symmetry quantum numbers are *not* conserved.

**ii) Unseen quarks** - All hadrons are made of quarks; yet, no individual quark can be seen.

These two puzzles have been with us for several decades, beginning with parity nonconservation in the fifties and $CP$ and time reversal violations in the sixties. They are perhaps of an equal profundity as the puzzles which faced our predecessors around the turn of the century.

## 1.1. Historical Remark

At the end of the last century, there were also two physics puzzles:

1. No absolute inertial frame (Michelson-Morley Experiment 1887),
2. Wave-particle duality (Planck's formula 1900).

These two seemingly esoteric problems struck classical physics at its very foundation. The first became the basis for Einstein's special theory of relativity and the second led to quantum mechanics. In this century, all the modern scientific and technological developments—*nuclear energy, atomic physics, molecular structure, lasers, x-ray technology, semiconductors, superconductors, supercomputers*—only exist because we have relativity and quantum mechanics. To humanity and to our understanding of nature, these are all-encompassing.

## 1.2. Vacuum As A Condensate

The puzzle of missing symmetries implies the existence of an entirely new class of fundamental forces, the one that is responsible for symmetry breaking. Of this new force, we know only of its existence, and very little else. Since the masses of particles break many of these symmetries, an understanding of the symmetry-breaking forces will lead to a comprehension of the origin of the masses of all known particles. One of the promising directions is the spontaneous symmetry-breaking mechanism[1] in which one assumes that

the physical laws remain symmetric, but the physical vacuum is not. If so, then the solution of this puzzle is closely connected to the structure of the physical vacuum; the excitations of the physical vacuum may lead to the discovery of Higgs-type mesons. The vacuum, though Lorentz invariant (therefore not aether), can be full of complexity.

In some textbooks, the second puzzle is often "explained" by using the analogy of the magnet. A magnet has two poles, north and south. Yet, if one breaks a bar magnet in two, each half becomes a complete magnet with two poles. By splitting a magnet open one will never find a single pole (magnetic monopole). However, in our usual description, a magnetic monopole can be considered as either a fictitious object (and therefore unseeable) or a real object but with exceedingly heavy mass beyond our present energy range (and therefore not yet seen). In the case of quarks, we believe them to be real physical objects and of relatively low masses (except the top quark); furthermore, their interaction becomes extremely weak at high energy. If so, why don't we ever see free quarks? This is, then, the real puzzle.

The current explanation of the quark confinement puzzle is again to invoke the vacuum. We assume the QCD vacuum to be a condensate of gluon pairs and quark-antiquark pairs so that it is a perfect color dia-electric[2] (i.e., color dielectric constant $\kappa = 0$). This is in analogy to the description of a superconductor as a condensate of electron pairs in BCS theory, which results in making the superconductor a perfect dia-magnet (with magnetic susceptibility $\mu = 0$). When we switch from QED to QCD we replace the magnetic field $\vec{H}$ by the color electric field $\vec{E}_{\text{color}}$, the superconductor by the QCD vacuum, and the QED vacuum by the interior of the hadron. As shown in Figure 1, the roles of the inside and the outside are interchanged. Just as the magnetic field is expelled outward from the superconductor, the color electric field is pushed into the hadron by the QCD vacuum, and that leads to color confinement, or the formation of hadrons (mesons, nucleons and other baryons). This situation is summarized in Table 1.

| QED superconductivity as a perfect dia-magnet | | QCD vacuum as a perfect color dia-electric |
|---|---|---|
| $\vec{H}$ | $\longleftrightarrow$ | $\vec{E}_{\text{color}}$ |
| $\mu_{\text{inside}} = 0$ | $\longleftrightarrow$ | $\kappa_{\text{vacuum}} = 0$ |
| $\mu_{\text{vacuum}} = 1$ | $\longleftrightarrow$ | $\kappa_{\text{inside}} = 1$ |
| inside | $\longleftrightarrow$ | outside |
| outside | $\longleftrightarrow$ | inside |

**Table 1.** Analogies between superconductivity and the QCD vacuum.

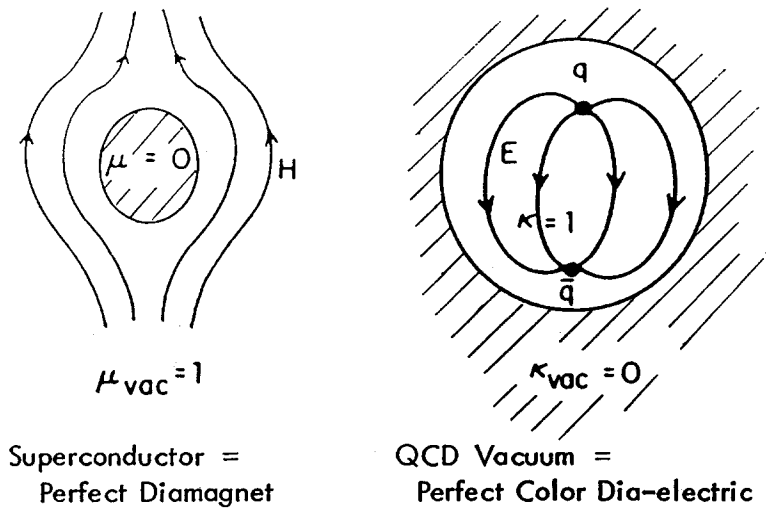


**Figure 1.** Superconductivity in QED vs. quark confinement in QCD.

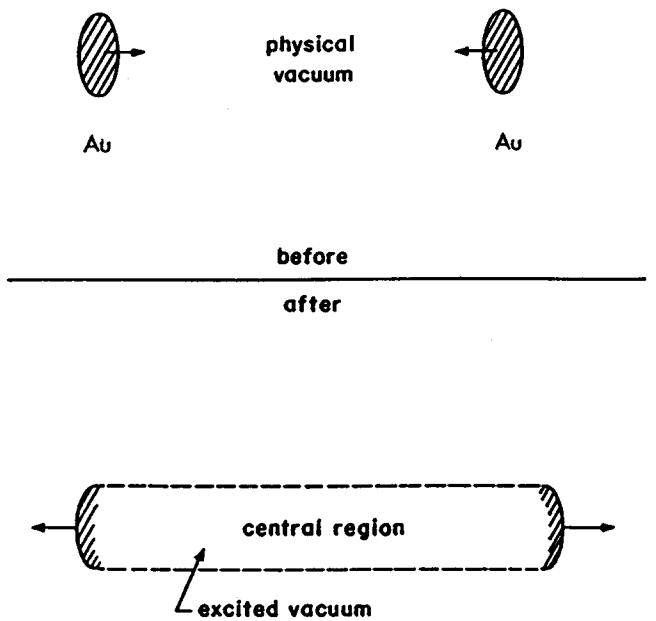


**Figure 2.** Vacuum excitation through relativistic heavy ion collisions.

QCD vacuum is, of course, Lorentz invariant. The product of its color dielectric constant times its color magnetic susceptibility is one, so that the velocity of light remains $c$. Thus, the hypothesis that the QCD vacuum is a perfect color dia-electric implies an infinite color magnetic susceptibility.

## 2. RHIC PHYSICS AND QCD

### 2.1. How To Excite the Vacuum?

In order to explore physics in this fundamental area, relativistic heavy ion collisions offer an important new direction.[3] The basic idea is to collide heavy ions, say gold on gold, at an ultra-relativistic region. Before the collision, the vacuum between the ions is the usual physical vacuum; at a sufficiently high energy, after the collision almost all of the baryon numbers are in the forward and backward regions (in the center-of-mass system). The central region is essentially free of baryons and, for a short duration, it is of a much higher energy density than the physical vacuum. Therefore, the central region could become the excited vacuum (Figure 2).

To realize this possibility, we need RHIC, the 100 GeV $\times$ 100 GeV (per nucleon) relativistic heavy ion collider at the Brookhaven National Laboratory, to explore the QCD vacuum.

### 2.2. Phase Diagram

Without any sophisticated theoretical analysis, we expect the QCD phase diagram to be of the form given by Figure 3, in which the ordinate is the thermal energy $kT$ and the abscissa is baryon number density in units of that in the normal nucleus. At AGS (11.6 GeV/nucleon) and at SPS (160 GeV/ nucleon) there are only fixed-target experiments. Consequently the center-of-mass energy is not likely to be high enough to create the quark gluon plasma.

Figure 4 gives the phase diagram[4] for pure lattice gauge QCD. The ordinate is entropy density/$T^3$ and the abscissa is $kT$. One finds a first-order phase transition at about 150 MeV thermal energy, leading from nearly zero entropy density to eight times that of a photon gas. (In pure gauge QCD there are only gluons which have eight color and two helicity states).

A realistic QCD calculation requires quarks. Figure 5(a) gives the 1990 version of the QCD phase diagram[5]. The abscissa denotes the mass of $u, d$ quarks times the lattice spacing $\ell$, and the ordinate is the mass of $s$ in the same units. There are five points, marked $A, B, C, D$ and $E$. Point $E$ refers to $m_{u,d} = m_s = \infty$; i.e., pure gauge QCD. As mentioned earlier, the result for pure gauge shows a first-order phase transition. Points $E, C$ and $D$ all lie on the upper boundary of the diagram ($m_s = \infty$). As of 1990, using a three-dimensional lattice of $16^3$ and a temperature (Euclidean time) division $N_T = 4$, the Columbia Group[5] found the result to be not a first-order phase transition. The extrapolation to $m_{u,d}$ to 0 should lead to a second-order phase transition. On the other hand, point $A$

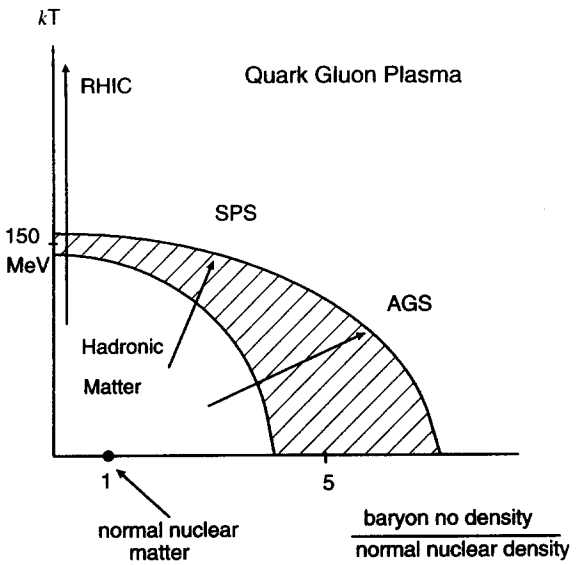


**Figure 3.** QCD Phase Diagram

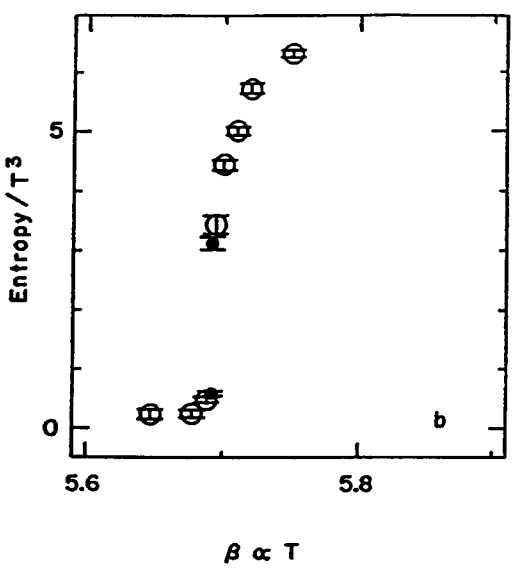


**Figure 4.** Phase transition (pure gauge QCD)

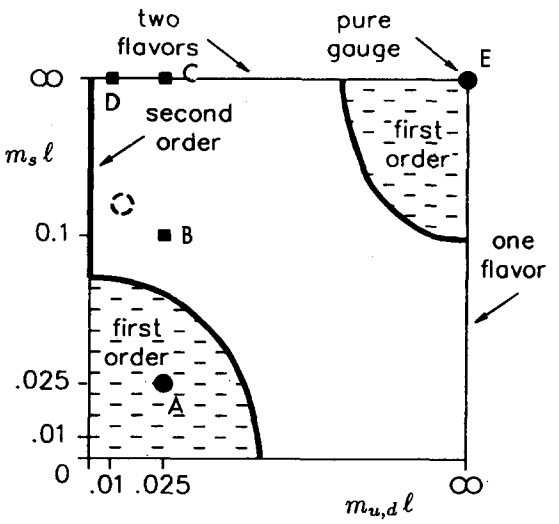


**Figure 5(a).** Finite-temperature QCD phase transition as a function of $m_{u,d}\ell$ and $m_s\ell$ on a $16^3 \times 4$ lattice.

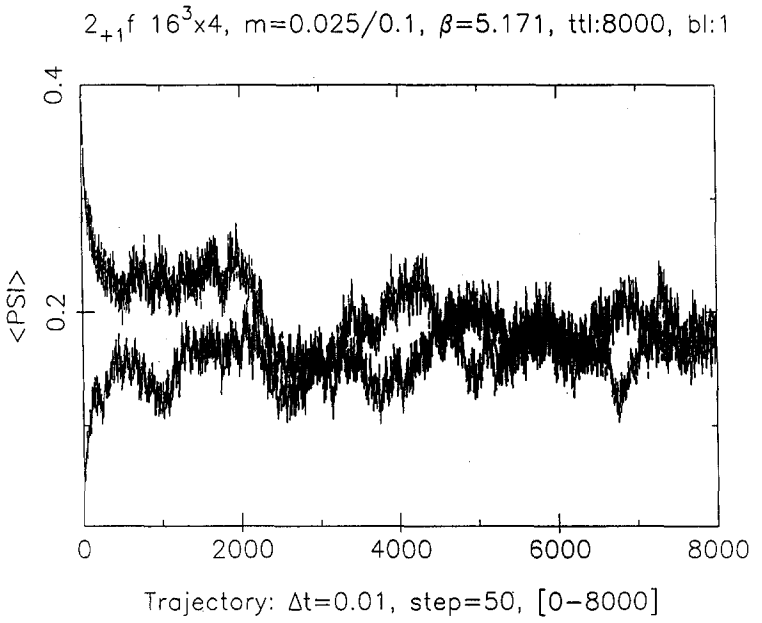


**Figure 5(b).** For $m_u = m_d = 0.025/\ell$, when $m_s$ increases from $0.25/\ell$ to $0.1/\ell$ the first-order phase transition disappears.

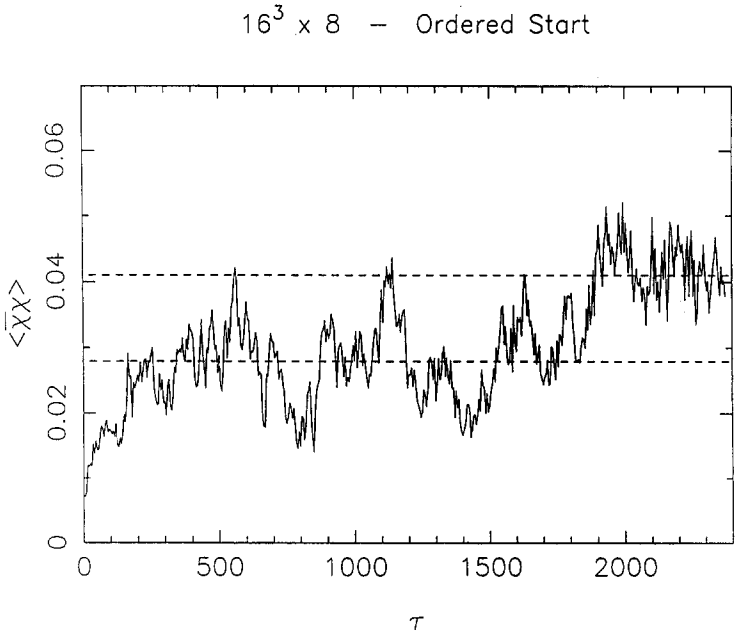


**Figure 6(a).** The cold start evolution at $\beta = 5.48$ for two light-flavor quarks.

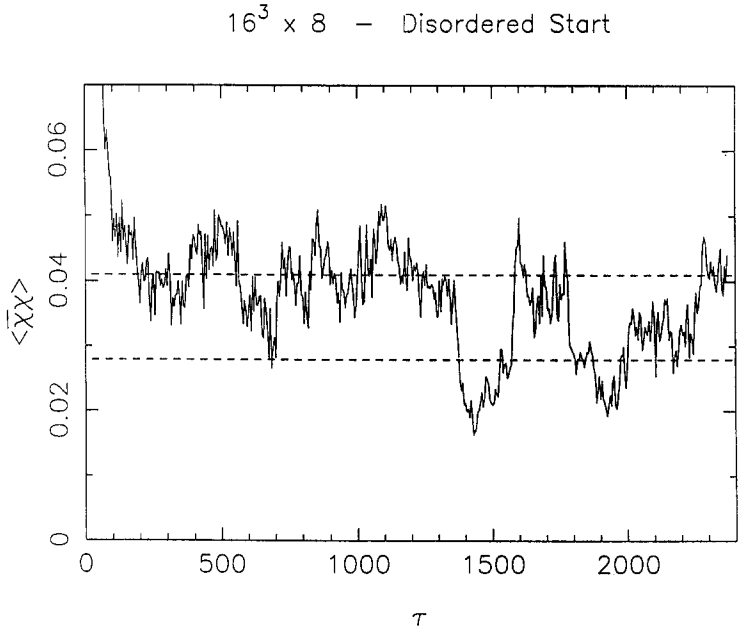


**Figure 6(b).** The hot start evolution at $\beta = 5.48$ for two light-flavor quarks.

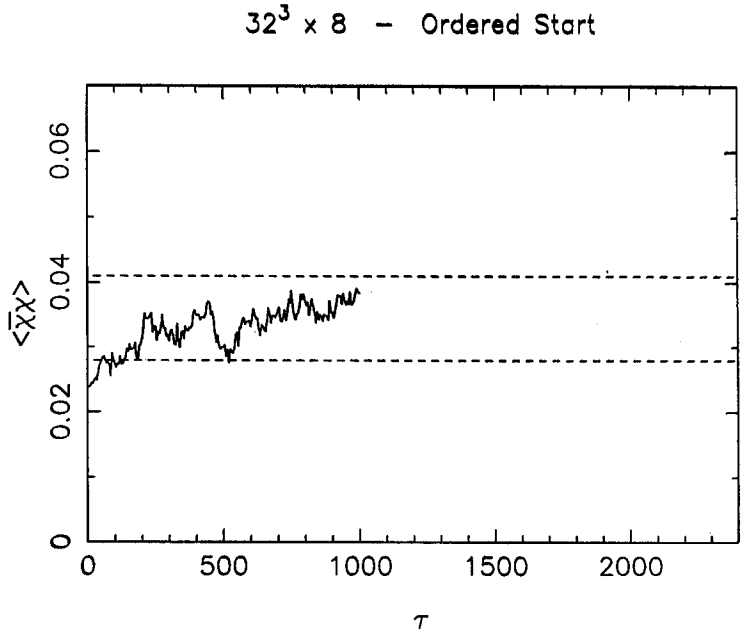


**Figure 7(a).** The cold start evolution at $\beta = 5.48$ for two light-flavor quarks.

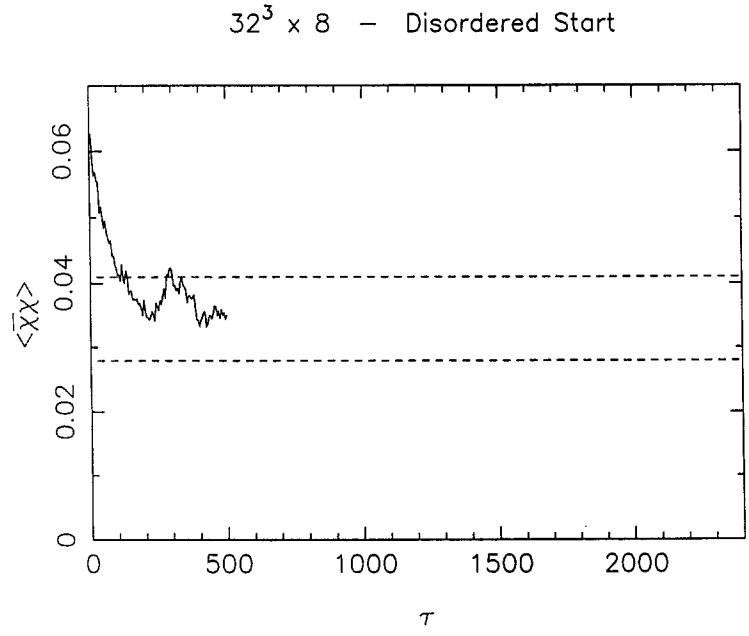


**Figure 7(b).** The hot start evolution at $\beta = 5.48$ for two light-flavor quarks.

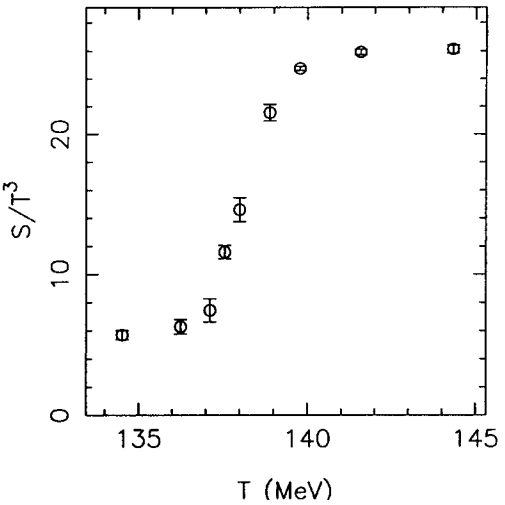


**Figure 8.** Entropy Density $S$ vs. temperature for two light-flavor quarks with $16^3 \times 4$ lattice ($m_u = m_d = 0.01/\ell$).

| CONTINUUM QCD | LATTICE QCD |
|---|---|
| ACTION $A = -\frac{1}{4}\int F_{\mu\nu}F_{\mu\nu}d^4x$ | $A = \sum_{\square} \frac{1}{2}$ trace $(1 - U_{\square}) +$ c.c. |
| ( $F_{\mu\nu}$ UNBOUNDED) | ( $U_{\square}$ BOUNDED) |
| NONCOMPACT $A$ | COMPACT $A$ |
| *Perturbative Series and Renormalization Group* | *Spurious Fermion Solutions and their removal* |
| Difficulties with | Difficulties with |
| confinement | pion mass |
| hadron spectra | dynamical processes |
| hadron distributions in dynamical processes | |

**Table 2.** Present Status of QCD

with $m_{u,d} = m_s = .025/\ell$ shows a first-order phase transition, but when $m_s$ increases to $0.1/\ell$ at point $B$ the first-order phase transition disappears, as shown in Figure 5(b). The boundary of the first-order region in Figure 5(a) is drawn freely.

Since the Columbia group under Norman Christ completed the 256-node dedicated parallel processor at the end of 1989, much work has been done to see how certain these conclusions are. By doubling the temperature slices from 4 to 8, and applying the $16^3$ lattice to the case of two light-flavor quarks (and an infinite $m_s$) the Columbia group first found a rather different conclusion from the 1990 phase diagram. As shown in Figures 6(a) and 6(b), the new results suggest a first-order transition[6] instead of second-order, which was obtained previously. But more surprises were yet to come.

Soon after, further intensive effort was made, maintaining the temperature slices at eight but increasing the spatial dimensions from $16^3$ to $32^3$. Unexpectedly, what looked like an indication of the first-order phase transition disappeared. The newer results[7], in Figures 7(a) and 7(b), show that the second-order phase transition for two light-flavor quarks is still the correct one. In other words, from 1990 to 1994 the theoretical evidence has turned $360^o$, from second-order phase transitions for two light-flavor quarks to first-order and then back to second-order. This shows how difficult these calculations are.

The Christ-Mawhinney group then concentrated on the physical manifestation of these differences, first order or second order, from an observational point of view. Extensive runs over different temperatures, concentrating on the two light-flavor quarks with $16^3 \times (N_t = 4)$, were made. The result still shows a second-order phase transition. However, as displayed in Figure 8, in terms of the physical observables entropy *vs.* temperature[8], it would be extremely difficult to tell experimentally whether we have a first-order or second-order phase transition.

### 2.3. Present Theoretical Limitations

Since QCD is the foundation of quark matter physics, it is important for us to examine critically our present understanding. Table 2 summarizes the basic actions of continuum and lattice QCD and the difficulties that we are facing. We emphasize that the present compact form[9] of lattice QCD is intrinsically different from the noncompact form of continuum QCD, except in the weak-coupling limit or when the lattice size equals zero. Both limits are difficult to achieve. In addition, for lattice QCD there is the problem of spurious fermion solutions, as will be discussed below.

## 3. A NEW THEORETICAL APPROACH

It is well known that the Dirac equation on a discrete lattice in $D$ dimension has $2^D$ degenerate solutions. The usual method of removing these spurious solutions encounters difficulties with chiral symmetry when the lattice spacing $\ell \neq 0$, as demonstrated by the persistent problem of pion and kaon masses. On the other hand, we recall that in any crystal in nature, all the electrons do move in a lattice and satisfy the Dirac equation; yet there is not a single physical result that has ever been entangled with a spurious fermion

solution. Therefore it should not be difficult to eliminate these unphysical elements.

On a discrete lattice, particles hop from point to point, whereas in a real crystal the lattice structure is embedded in a continuum and electrons move continuously from lattice cell to lattice cell. In a discrete system, the lattice functions are defined only on individual points (or links, as in the case of gauge fields). However, in a crystal the electron state vector is represented by the Bloch wave functions which are continuous functions in $\vec{r}$, and herein lies one of the essential differences.

In this new approach we shall expand the field operator in terms of a suitably chosen complete set of orthonormal Bloch functions

$$\{ f_n(\vec{K} \,|\, \vec{r}) \} \tag{1}$$

where $\vec{K}$ denotes the Bloch wave number restricted to the Brillouin zone, and $n$ labels the different bands. Thus, $e^{-i\vec{K}\cdot\vec{r}} f_n(\vec{K} \,|\, \vec{r})$ has the periodicity of the lattice. The lattice approximation is then derived by either restricting it to only one band (say, $n = 0$), or to a few appropriately defined low-lying bands. Since the inclusion of all bands *is* the original continuum problem, there is a natural connection between the lattice and the continuum in this method. By including the contributions due to more and more bands, one can systematically arrive at the exact continuum solution from the lattice approximation, as we shall see. There is a large degree of freedom in choosing the Bloch functions (1.1), as the original continuum theory has no crystal structure. These extra degrees of freedom are analogous to gauge fixing; the final answer to the continuum problem is independent of the particular choice of Bloch functions.

### 3.1. Spurious Lattice Fermion Solutions

To see the origin of the spurious lattice fermion solutions, we may consider the replacement of the continuum equation $-i\,\partial\psi\,/\,\partial x = p\psi$ by its discrete form in one space dimension:

$$-\frac{i}{2\ell}\,(\psi_{j+1} - \psi_{j-1}) \;=\; p_L\,\psi_j \tag{2}$$

where $\psi_j$ is the value of $\psi$ at the $j^{th}$ site. The above equation can also be derived by setting the derivative $\partial\,/\,\partial\psi_j$ of the discrete bilinear form

$$B_L \;\equiv\; \frac{1}{2}\left[-i\sum_j \psi_j^\dagger(\psi_{j+1} - \psi_j)\,/\,\ell + \text{h.c.}\right] \tag{3}$$

to be zero at a constant $\sum_j \psi_j^\dagger\,\psi_j$. The lattice-eigenvalue $p_L$ is given by

$$p_L \;=\; \frac{1}{\ell}\,\sin K\ell \tag{4}$$

where

$$K\ell \;\equiv\; \theta \tag{5}$$

is between $-\pi$ and $\pi$. The spurious solution refers to the zero ($p_L(\theta) = 0$) at $\theta = \pi$ (which is the same as $\theta = -\pi$). This is a special case of the Nielsen-Ninomiya theorem[10]: For any continuous and periodic function $p_L(\theta)$, if as $\theta \to 0$ $p_L(\theta) \to K = \theta/\ell$, then because of the periodicity $p_L(\theta) = p_L(\theta + 2\pi)$, there must be another zero of $p_L(\theta)$ for $\theta$ between 0 and $2\pi$. For a $D$-dimension cubic lattice, the corresponding wave function is a product function, the number of spurious solutions becomes $2^D$.

### 3.2. Elimination of Spurious Lattice Fermion Solutions[11]

We expand the continuum wave function $\psi(x)$ in terms of (1), in which the zeroth band ($n = 0$) is simply the linear interpolation of the discrete values $\{\psi_j\}$; i.e., in the zeroth-band approximation

$$\psi(x) = \sum_j \psi_j \Delta(x - j\ell) \tag{6}$$

where

$$\Delta(x) = \begin{cases} 1 - \frac{|x|}{\ell} & \text{for } |x| < \ell \\ 0 & \text{otherwise.} \end{cases}$$

Thus, at $x = j\ell$, $\psi(x) = \psi_j$. Substitute (6) into the continuum bilinear form

$$B(\psi(x)) \equiv -i \int \psi(x)^\dagger \frac{d\psi(x)}{dx}\, dx. \tag{7}$$

Setting $\partial B / \partial \psi_j = 0$ at a constant $\int \psi^\dagger \psi\, dx$, we find

$$\psi_j \propto e^{i\theta j}$$

with $\theta$ given by (5). Correspondingly, the zeroth-band Bloch function is

$$f_0(K\,|\,x) = \sqrt{\frac{3}{N\ell(2+\cos\theta)}} \sum_j e^{i\theta j}\, \Delta(x - j\ell) \tag{8}$$

where $N$ is the total number of lattice sites. It is not difficult to construct from $f_0(K\,|\,x)$ and the Fourier series a complete set of Bloch functions (1), which satisfy

$$\int_0^{N\ell} f_n(K\,|\,x)^*\, f_{n'}(K'\,|\,x)\, dx = \delta_{nn'}\, \delta_{KK'}. \tag{9}$$

Let

$$\beta_n \equiv -i \int f_n(K\,|\,x)^* \frac{\partial}{\partial x} f_n(K\,|\,x)\, dx. \tag{10}$$

We find for $n = 0$

$$\beta_0 = \frac{3\sin\theta}{2+\cos\theta} \tag{11}$$

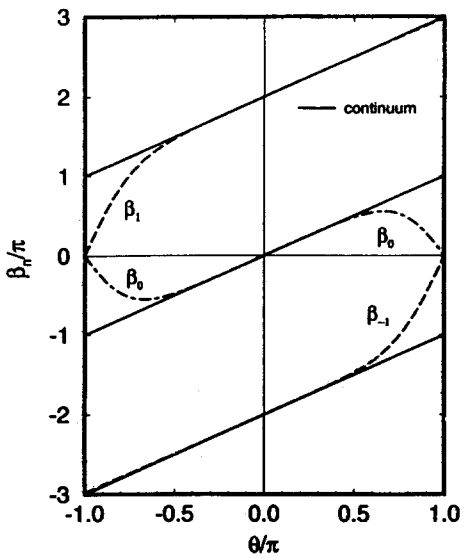


**Figure 9.** The dash-dot line gives $\beta_0 = 3\sin\theta/(2+\cos\ell)$ vs $\theta = K\ell$ and the dashed lines denote $\beta_{-1}$ and $\beta_1$ defined by (10). The solid lines are the continuum free-particle spectrum $p\ell = K\ell + 2\pi m$ vs $\theta$, with $m = 0$ and $\pm 1$.

which, like (4), has a spurious zero solution at $\theta = \pi$.

If we substitute the full expansion

$$\psi(x) = \sum_n \sum_k q_n(K)\, f_n(K\,|\,x) \tag{12}$$

into (7), then $\delta B/\delta\psi(x) = 0$ at a constant $\int \psi^\dagger\psi\, dx$ gives $-i\,\partial\psi/\partial x = px$ where

$$p = K + \frac{2\pi m}{\ell} \tag{13}$$

with $K$ given by (5) and $m = \cdots, -1, 0, 1, \cdots$.

In Figure 9, the abscissa is $\theta/\pi = K\ell/\pi$, the solid line gives the exact continuum value $p\ell/\pi$ and the different segments correspond to $m = -1, 0, 1$. The dashed line segments are the corresponding $\beta_n/\pi$, defined by (10). For $|n| > 1$, each $\beta_n$ deviates from the exact continuum result (13) within $< 1\%$. For $|n| \leq 1$, we see that $\beta_0$ and $\beta_{-1}$ are both 0 at $\theta = \pi$; likewise $\beta_0$ and $\beta_1$ are both 0 at $\theta = -\pi$. Thus, the spurious solutions also extend to $n = \pm 1$ bands. This additional unwanted degeneracy makes it easy to remove all spurious solutions, as we shall see.

Because $f_0(K\,|\,x)$ and $f_1(K\,|\,x)$ are not eigenfunctions of $-i\partial\,/\,\partial x$, the degeneracy between $\beta_0$ and $\beta_{-1}$ at $\theta = \pi$ can be removed by considering the off-diagonal elements of $-i\,\partial\,/\,\partial x$. At $\theta = \pi - \epsilon$ where $\epsilon$ is a positive infinitesimal, we may consider only two bands, $n = 0$ and $-1$; in this subspace the operator $-i\partial\,/\,\partial x$ becomes the following $2 \times 2$ matrix:

$$\begin{pmatrix} 3\epsilon & \sqrt{10}\,/\,\ell \\ \sqrt{10}\,/\,\ell & -5\epsilon \end{pmatrix}. \tag{14}$$

As $\epsilon \to 0$, its eigenvalues are

$$\pm\sqrt{10}\,/\,\ell \;=\; \pm 1.006 \times \pi\,/\,\ell. \tag{15}$$

Similar considerations apply to $\theta = -\pi$ by taking into account the coupling between $n = 0$ and $n = 1$ band. Thus, by taking into account only $n = 0$ and $\pm 1$, we have removed all spurious zero-mode solutions and, in addition, the result differs from the exact continuum value by less than a few tenths of a percent for the entire range.

### 3.3. Noncompact Lattice QCD

In order to extend the above considerations to QCD we have to construct an appropriate complete set of Bloch wave functions that is compatible with the gauge-fixing condition. Once that is done, the restriction to the $0^{th}$ band ($n = 0$) gives a noncompact formulation[12] of lattice QCD. The exact continuum theory can be reached through the inclusion of all $n = 0$ and $n \neq 0$ bands, without requiring the lattice size $\ell \to 0$. This makes it possible, at a nonzero $\ell$, for the lattice coupling $g_\ell$ to act as the renormalized continuum coupling. All physical results in the continuum are, of course, independent of $\ell$. We hope, with this new formulation, it may be possible to handle the low-lying meson masses as well as dynamical RHIC processes in the future.

### 3.4. Looking Ahead

We are now at the beginning of 1995, and soon it will be the end of the century. We may ask what will be the legacy that we give to the next generation in the next century? The physicists at the end of the nineteenth century had a glimpse of a new vista: the existence of exciting and unexplored fundamental areas. Today we are confronted with two similarly profound puzzles of modern physics.

Through RHIC we may be able to alter the physical vacuum. If the vacuum is indeed the underlying cause for the two puzzles of missing symmetry and quark confinement in the microscopic world of particle physics, it must also have been actively responsive to the macroscopic distribution of matter and energy in the universe. Because the vacuum is everywhere and forever these two, the micro and the macro, have to be linked. Neither can be considered a separate entity.

## REFERENCES

1. For a history of this subject, see Y. Nambu, Fields and Quanta **1**, 33 (1970).

2. T. D. Lee, Phys.Rev. D**19**, 1802 (1979).

3. T.D. Lee and G.C. Wick, Phys.Rev. D**9**, 2291 (1974); T.D. Lee, "A Possible New Form of Matter", in *Report of the Workshop on BeV/Nucleon Collisions of Heavy Ions–How and Why*, Bear Mountain 1974 (BNL No. 50445), 1.

4. F. R. Brown, N. H. Christ, Y. F. Deng, M. S. Gao and T. J. Woch, Phys.Rev.Lett. **61**, 2058 (1988).

5. F. R. Brown, F. P. Butler, H. Chen, N. H. Christ, Z. Dong, W. Schaffer, L. I. Unger and A. Vaccarino, Phys.Rev.Lett. **65**, 2491 (1990).

6. R. D. Mawhinney, "QCD Thermodynamics at $N_t = 8$", Nucl.Phys.B (Proc.Suppl.) **30**, 331 (1993).

7. D. Zhu, "QCD Phase Transition for $N_t = 8$ on $16^3$ and $32^3$ Volumes", Nucl.Phys.B (Proc.Suppl.) **34**, 286 (1994).

8. S. Chandrasekharan, "Critical Behavior of the Chiral Condensate at the QCD Phase Transition", to appear in Nucl.Phys.B (Proc.Suppl.), proceedings of *Lattice '94*.

9. K. Wilson, Phys.Rev. D**10**, 2455 (1974); J. B. Kogut and L. Susskind, Phys.Rev. D**11**, 395 (1975). M. Creutz, Phys.Rev. D**21**, 2308 (1980).

10. H. B. Nielsen and M. Ninomiya, Nucl.Phys. B**185**, 20 (1981); **193**, 173 (1981).

11. R. Friedberg, T. D. Lee and Y. Pang, J.Math.Phys. **35**, 5600 (1994).

12. R. Friedberg, T. D. Lee, Y. Pang and H. C. Ren, "Noncompact Lattice Formulation of Gauge Theories", Columbia University Preprint CU-TP-662.